

A HYBRID INVERSION SCHEME OF MARKOV-CHAIN MONTE CARLO AND ITERATIVE METHODS FOR DIFFUSE OPTICAL TOMOGRAPHY

YU JIANG, MANABU MACHIDA, AND GEN NAKAMURA

ABSTRACT. Diffuse optical tomography is formulated as inverse coefficient problems for the diffusion equation. Iterative inversion schemes such as the Levenberg-Marquardt algorithm are known to fail when initial guesses are not close to the true value of the coefficient to be reconstructed. In this paper, we investigate how this weakness of iterative schemes is overcome by the use of Monte Carlo. We present a toy model of diffuse optical tomography for which the Levenberg-Marquardt algorithm fails to work but the Metropolis-Hastings Markov chain Monte Carlo works. We show that our proposed hybrid scheme solves the inverse problem efficiently by preparing a good initial guess by Monte Carlo and then computing the reconstructed value with the Levenberg-Marquardt algorithm starting from the found initial guess.

1. INTRODUCTION

Inverse diffusion problems appear when we try to find the structure of optical properties of a highly-scattering random medium such as biological tissue using light propagating in the medium of interest. Since the energy density of light in such random media is governed by the diffusion equation in the macroscopic regime, in which the propagation distance of light is much larger than the transport mean free path, inverse problems for the diffusion equation are concerned. Diffuse optical tomography is a medical imaging modality which obtains tomographic images using infrared light. In addition to the ability of finding tumors such as women's breast cancer [1], function such as brain activity [2] can be studied with diffuse optical tomography [3, 4, 5].

When the absorption coefficient, diffusion coefficient, or both are reconstructed, diffuse optical tomography is formulated as coefficient inverse problems of the diffusion equation. Newton-type iterative methods such as the Levenberg-Marquardt algorithm are commonly used to solve related inverse problems. See [6, 7] for commonly used numerical techniques for diffuse optical tomography. For these numerical methods to work, it is important to use a good initial guess for the initial value of the iteration. Therefore the knowledge of optical properties such as the diffusion coefficient and absorption coefficient of the background tissue is necessary. However, in-vivo measurements have to be done in a small region of order 1 mm to investigate optical properties of each organ. Hence although this is a long-standing issue [8, 9, 10], optical properties in biological tissue are not yet fully understood [11]. Therefore sometimes it is not easy to set good initial guesses.

Solving inverse problems by the Bayesian approach has been sought as an alternative way of obtaining reconstructed images. The Bayesian inversion with the Metropolis-Hastings Markov chain Monte Carlo was used in [12, 13]. In [14], the Bayesian approach was used for diffuse optical tomography. Using the Bayesian approach, optical properties of the human head (scalp, skull, and brain) were investigated [15]. For the Markov chain Monte Carlo (MCMC), the reader is referred to the textbooks by Robert and Casella [16], by Liu [17], and by Nakamura and Potthast [18].

Although the Markov-chain Monte Carlo approach is in principle able to escape from local minima, it is computationally time consuming and moreover is difficult to find precise values of unknown quantities due to statistical error. In this paper, we propose a hybrid numerical scheme of Markov-chain Monte Carlo and iterative methods. By developing a toy model for diffuse optical tomography, we examine when the iterative scheme fails by being trapped by a local minimum and how the Markov-chain Monte Carlo approach is able to escape from such local minima. Even though practical models have a cost function with different local minima, the global minimum often cannot be found. The toy model devised in this paper is simple enough to explicitly understand the structure of the cost function, which has a local minimum and a global minimum. We propose a hybrid scheme in which the Markov-chain Monte Carlo is first used to solve the inverse problem, and then an iterative method is used after the burn-in time to determine the value of an unknown quantity with an initial guess from the Markov-chain Monte Carlo.

2. DIFFUSION EQUATION

2.1. Half space in two dimensions. Let us obtain approximate solutions of the diffusion equation with spatially varying absorption coefficient in the two-dimensional half space using the Born approximation.

Throughout this paper, Ω denotes the half space in \mathbb{R}^2 , i.e., $\Omega = \mathbb{R}_+^2 := \{x \in \mathbb{R}^2; x_1 \in \mathbb{R}, x_2 > 0\}$, and $\partial\Omega$ is the boundary of Ω , i.e., the x_1 -axis. Let us define

$$\Omega_T := \Omega \times (0, T), \quad \partial\Omega_T := \partial\Omega \times (0, T),$$

where positive constant T denotes the measurement time. We consider the following diffusion equation.

$$\begin{cases} (\partial_t - \gamma\Delta + b(x)) u(x, t; x^i) = 0, & (x, t) \in \Omega_T, \\ \ell\partial_\nu u(x, t; x^i) + u(x, t; x^i) = \delta(x - x^i)\delta(t), & (x, t) \in \partial\Omega_T, \\ u(x, t; x^i) = 0, & x \in \Omega, \quad t = 0, \end{cases}$$

where $\Delta = \partial_{x_1}^2 + \partial_{x_2}^2$, $\nabla = {}^t(\partial_{x_1}, \partial_{x_2})$, and $\partial_\nu = \nu \cdot \nabla = -\partial_{x_2}$ with the outer unit normal ν . Here $x^i \in \partial\Omega$ is the position of the i th source ($i = 1, 2, \dots, M_s$). We assume that γ is a positive constant and ℓ is a nonnegative constant. Let us write the absorption coefficient $b(x) \geq 0$ as

$$b(x) = b_0 + \delta b(x),$$

where b_0 is a constant and the perturbation $\delta b(x)$ spatially varies.

2.2. Rytov approximation. Let us assume that δb is small. Within the (first) Born approximation u is given by

$$u(x, t; x^i) = u_0(x, t; x^i) - \int_{\Omega_T} G(x, t; y, s) \delta b(y) u_0(y, s; x^i) dy ds,$$

where $u_0(x, t; x^i)$ is the solution to the following diffusion equation.

$$\begin{cases} (\partial_t - \gamma \Delta + b_0) u_0(x, t; x^i) = 0, & (x, t) \in \Omega_T, \\ \ell \partial_\nu u_0(x, t; x^i) + u_0(x, t; x^i) = \delta(x - x^i) \delta(t), & (x, t) \in \partial \Omega_T, \\ u_0(x, t; x^i) = 0, & x \in \Omega, \quad t = 0, \end{cases}$$

and the Green's function $G(x, t; y, s)$ satisfies

$$\begin{cases} (\partial_t - \gamma \Delta + b_0) G = \delta(x - y) \delta(t - s), & (x, t) \in \Omega_T, \\ \ell \partial_\nu G + G = 0, & (x, t) \in \partial \Omega_T, \\ G = 0, & x \in \Omega, \quad t = 0. \end{cases}$$

We obtain (see Appendix A)

$$\begin{aligned} u_0(x, t; x^i) &= \frac{e^{-b_0 t}}{\sqrt{4\pi\gamma t}} e^{-\frac{(x_1 - x_1^i)^2 + x_2^2}{4\gamma t}} \\ &\times \left[\frac{2}{\sqrt{4\pi\gamma t}} - \frac{1}{\ell} e^{\left(\frac{x_2 + 2\gamma t/\ell}{\sqrt{4\gamma t}}\right)^2} \operatorname{erfc}\left(\frac{x_2 + 2\gamma t/\ell}{\sqrt{4\gamma t}}\right) \right]. \end{aligned}$$

Furthermore,

$$\begin{aligned} G(x, t; y, s) &= \frac{e^{-b_0(t-s)}}{\sqrt{4\pi\gamma(t-s)}} e^{-\frac{(x_1 - y_1)^2}{4\gamma(t-s)}} \\ &\times \left[\frac{1}{\sqrt{4\pi\gamma(t-s)}} \left(e^{-\frac{(x_2 - y_2)^2}{4\gamma(t-s)}} + e^{-\frac{(x_2 + y_2)^2}{4\gamma(t-s)}} \right) \right. \\ &\left. - \frac{1}{\ell} e^{-\frac{(x_2 + y_2)^2}{4\gamma(t-s)}} e^{\left(\frac{x_2 + y_2 + 2\gamma(t-s)/\ell}{\sqrt{4\gamma(t-s)}}\right)^2} \operatorname{erfc}\left(\frac{x_2 + y_2 + 2\gamma(t-s)/\ell}{\sqrt{4\gamma(t-s)}}\right) \right], \end{aligned}$$

for $t \geq s$ and $G(x, t; y, s) = 0$ when $t < s$. The complementary error function is defined by $\operatorname{erfc}(z) = (2/\sqrt{\pi}) \int_z^\infty \exp(-t^2) dt$.

To obtain the expression of the Rytov approximation, we introduce ψ_0, ψ_1 as [19]

$$u_0 = e^{\psi_0}, \quad u = e^{\psi_0 + \psi_1}.$$

By plugging the above expressions of u, u_0 into the Born approximation and keeping terms of $O(\delta b)$, we obtain

$$\begin{aligned} e^{\psi_1} &= 1 - e^{-\psi_0} \int_{\Omega_T} G(x, t; y, s) \delta b(y) u_0(y, s; x^i) dy ds \\ &= \exp \left[-e^{-\psi_0} \int_{\Omega_T} G(x, t; y, s) \delta b(y) u_0(y, s; x^i) dy ds \right]. \end{aligned}$$

That is, we have

$$\psi_1 = -u_0 \int_{\Omega_T} G(x, t; y, s) \delta b(y) u_0(y, s; x^i) dy ds.$$

The (first) Rytov approximation is thus given by

$$u(x, t; x^i) = u_0(x, t; x^i) \exp \left[-\frac{1}{u_0(x, t; x^i)} \int_{\Omega_T} G(x, t; y, s) \delta b(y) u_0(y, s; x^i) dy ds \right]. \quad (1)$$

Although both of the Born and Rytov approximations are the first-order approximation, the superiority of the latter has been discussed [20, 21].

3. DIFFUSE LIGHT

3.1. Absorption inhomogeneity. We detect the out-going light from each source on the boundary at x^j ($j = 1, 2, \dots, M_d$). During $0 < t < T$, measurements are performed at times t^k ($k = 1, 2, \dots, M_t$). The measured data y_{ijk} usually contain some noise e_{ijk} . That is, we can write

$$y_{ijk} = u(x^j, t^k; x^i)(1 + e_{ijk}), \quad (2)$$

where $u(x^j, t^k; x^i)$ is given in (1). We assume the Gaussian noise given by

$$e_{ijk} \sim \mathcal{N}(0, \sigma_e^2),$$

where $\mathcal{N}(0, \sigma_e^2)$ is the normal distribution with mean 0 and variance σ_e^2 . We set $\sigma_e = 0.03$ (3% noise). Let us suppose that the inhomogeneity $\delta b(x)$ is given by

$$\delta b(x) = \eta f_a(x_1) \delta(x_2 - x_{02}), \quad (3)$$

where η, x_{02} are positive constants. Here, $f_a(x_1)$ is given by

$$f_a(x_1) = \left[a^3 + 3 \left(1 + \frac{\tanh x_1^2}{10} \right) a^2 \right] (1 - \tanh x_1^2), \quad (4)$$

where $a > 1.1$ is a constant. In this paper, we assume that in (3), η, x_{02} are known but only a is unknown. For a fixed x_1 , the function $f_a(x_1)$ has a local minimum at $a = 0$ with height $f_0(x_1) = 0$ and the local maximum at $a = -2 \left(1 + \frac{\tanh x_1^2}{10} \right)$ with height $f_a(x_1) = 4 \left(1 + \frac{\tanh x_1^2}{10} \right)^3 (1 - \tanh x_1^2)$. We note that $f_{1.1}(x_1)$ is larger than the local maximum. On the other hand, as is shown in Fig. 1, the function $f_a(x_1)$ has one peak at $x_1 = 0$ and the maximum value is $f_a(0) = a^2(a + 3)$, f_a monotonically decays for $|x_1| > 0$, and $f_a \rightarrow 0$ as $|x_1| \rightarrow \infty$.

To numerically calculate $u(x, t; x^i)$, we begin by defining

$$g(x_2, t; y_2, s) = \frac{1}{4\pi\gamma(t-s)} e^{-\frac{(x_2+y_2)^2}{4\gamma(t-s)}} \left[1 + e^{\frac{(x_2+y_2)^2 - (x_2-y_2)^2}{4\gamma(t-s)}} - \frac{\sqrt{4\pi\gamma(t-s)}}{\ell} e^{\left(\frac{x_2+y_2}{2\sqrt{\gamma(t-s)}} + \frac{\sqrt{\gamma(t-s)}}{\ell} \right)^2} \operatorname{erfc} \left(\frac{x_2+y_2}{2\sqrt{\gamma(t-s)}} + \frac{\sqrt{\gamma(t-s)}}{\ell} \right) \right].$$

Then we have

$$\int_0^T G(x, t; y, s) u_0(y, s) ds = e^{-b_0 t} \int_0^t e^{-\frac{(x_1-y_1)^2}{4\gamma(t-s)}} e^{-\frac{(y_1-x_1^i)^2}{4\gamma s}} g(x_2, t; y_2, s) g(y_2, s; 0, 0) ds.$$

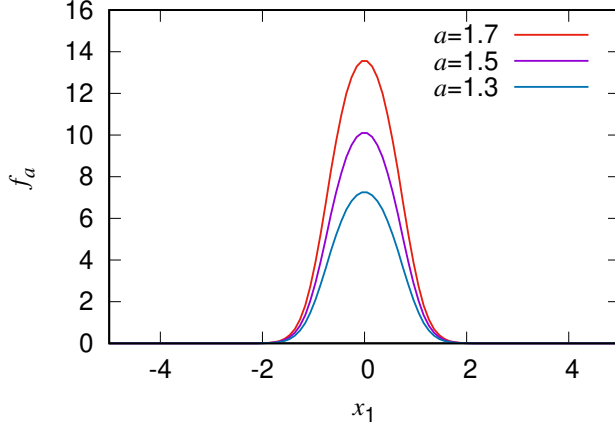


FIGURE 1. The function $f_a(x_1)$ in (4) is plotted for $a = 1.3, 1.5$, and 1.7 .

Therefore we obtain

$$\begin{aligned} u(x, t; x^i) &= u_0(x, t; x^i) \exp \left[-\frac{e^{-b_0 t}}{u_0(x, t; x^i)} \int_{\Omega} \delta b(y) \right. \\ &\quad \times \left. \left(\int_0^t e^{-\frac{(x_1 - y_1)^2}{4\gamma(t-s)}} e^{-\frac{(y_1 - x_1^i)^2}{4\gamma s}} g(x_2, t; y_2, s) g(y_2, s; 0, 0) ds \right) dy \right]. \end{aligned}$$

By substituting δb in (3), which contains the unknown parameter \bar{a} , we can express the energy density as

$$\begin{aligned} u(x^j, t^k; x^i; a) &= u(x^j, t^k; x^i) \\ &= u_0(x^j, t^k; x^i) \exp \left[-\frac{\eta e^{-b_0 t^k}}{u_0(x^j, t^k; x^i)} \int_0^{t^k} g(0, t^k; x_{02}, s) g(x_{02}, s; 0, 0) \right. \\ &\quad \times \left. \left(\int_{-\infty}^{\infty} f_a(y_1) e^{-\frac{(x_1^j - y_1)^2}{4\gamma(t^k-s)}} e^{-\frac{(y_1 - x_1^i)^2}{4\gamma s}} dy_1 \right) ds \right]. \end{aligned}$$

The energy density u is more explicitly written as

$$\begin{aligned} u(x^j, t^k; x^i; a) &= u_0(x^j, t^k; x^i) \exp \left[-\frac{\eta e^{-b_0 t^k}}{(2\pi\gamma)^2 u_0(x^j, t^k; x^i)} \int_0^{t^k} \frac{1}{(t^k - s)s} e^{-\frac{x_{02}^2}{4\gamma(t^k-s)}} e^{-\frac{x_{02}^2}{4\gamma s}} \right. \\ &\quad \times \left[1 - \frac{\sqrt{\pi\gamma(t^k-s)}}{\ell} e^{\left(\frac{x_{02}}{2\sqrt{\gamma(t^k-s)}} + \frac{\sqrt{\gamma(t^k-s)}}{\ell} \right)^2} \operatorname{erfc} \left(\frac{x_{02}}{2\sqrt{\gamma(t^k-s)}} + \frac{\sqrt{\gamma(t^k-s)}}{\ell} \right) \right] \\ &\quad \times \left[1 - \frac{\sqrt{\pi\gamma s}}{\ell} e^{\left(\frac{x_{02}}{2\sqrt{\gamma s}} + \frac{\sqrt{\gamma s}}{\ell} \right)^2} \operatorname{erfc} \left(\frac{x_{02}}{2\sqrt{\gamma s}} + \frac{\sqrt{\gamma s}}{\ell} \right) \right] \\ &\quad \times \left. \left(\int_{-\infty}^{\infty} \left[a^3 + 3 \left(1 + \frac{\tanh y_1^2}{10} \right) a^2 \right] (1 - \tanh y_1^2) e^{-\frac{(x_1^j - y_1)^2}{4\gamma(t^k-s)}} e^{-\frac{(y_1 - x_1^i)^2}{4\gamma s}} dy_1 \right) ds \right], \quad (5) \end{aligned}$$

where

$$u_0 = \frac{e^{-b_0 t^k}}{2\pi\gamma t^k} e^{-\frac{(x_1^j - x_1^i)^2}{4\gamma t^k}} \left[1 - \frac{\sqrt{\pi\gamma t^k}}{\ell} e^{\left(\frac{\sqrt{\gamma t^k}}{\ell}\right)^2} \operatorname{erfc}\left(\frac{\sqrt{\gamma t^k}}{\ell}\right) \right].$$

For the numerical evaluation of erfc , we note that

$$\operatorname{erfc}(\xi) \simeq \frac{e^{-\xi^2}}{\sqrt{\pi}\xi} \left[1 - \frac{1}{2\xi^2} + \frac{3}{(2\xi^2)^2} - \frac{15}{(2\xi^2)^3} + \dots \right],$$

for large $\xi > 0$.

3.2. Forward data. We place sources S_1, S_2 ($M_s = 2$) and detectors D_1, D_2, D_3 ($M_d = 3$) on the x_1 -axis as shown in Fig. 2. We assume the following physiological parameters.

$$\gamma = \frac{c}{3\mu'_s} = 0.07 \text{ mm}^2/\text{ps}, \quad b_0 = c\mu_a = 0.004 \text{ mm}^{-1}, \quad \ell = 2 \text{ mm}, \quad (6)$$

where $c = 0.3/1.37$ is the speed of light in the medium, $\mu'_s = 1 \text{ mm}^{-1}$ is the reduced scattering coefficient, and $\mu_a = 0.02 \text{ mm}^{-1}$ is the absorption coefficient for the radiative transport equation. For δb in (3), we put

$$\eta = 300, \quad a = 1.5, \quad x_{02} = 5. \quad (7)$$

Finally, we prepare y_{ijk} in (2) by adding noise after computing (5). We add 3% Gaussian noise. The resulting y_{ijk} are shown from Figs. 3 and 4.

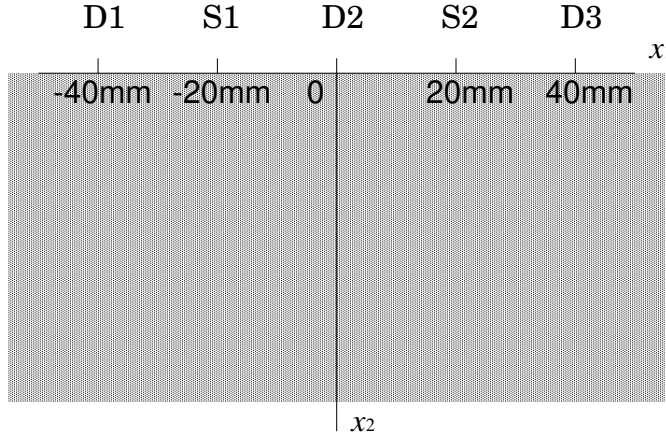


FIGURE 2. Sources and detectors on the boundary. On the x_1 -axis, the sources are at $\pm 20 \text{ mm}$ and detectors are at $\pm 40 \text{ mm}$, 0 mm .

4. INVERSE PROBLEMS BY ITERATIVE SCHEMES

Let $U \in \mathbb{R}^{M_s M_d M_t}$ be the vector from measurements and $F(a) \in \mathbb{R}^{M_s M_d M_t}$ be the vector from simulation, i.e.,

$$\begin{aligned} \{U\}_{ijk} &= y_{ijk} = u(x^j, t^k; x^i; \bar{a})(1 + e_{ijk}) \\ \{F(a)\}_{ijk} &= u(x^j, t^k; x^i; a), \end{aligned}$$

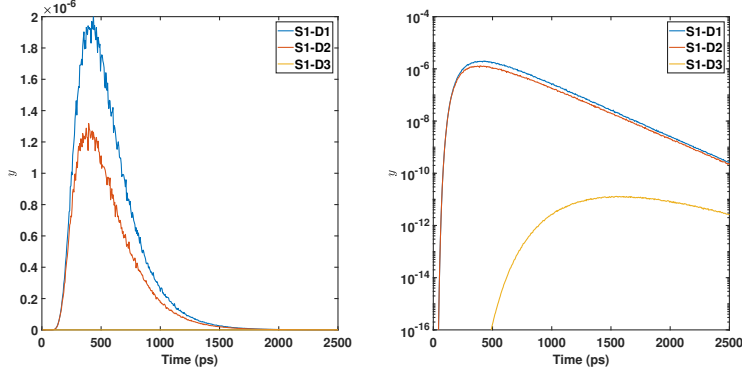


FIGURE 3. The energy density y of u given in (5) with 3% noise is calculated at D_1 (blue), D_2 (orange), and D_3 (yellow) when light is emitted from the source S_1 .

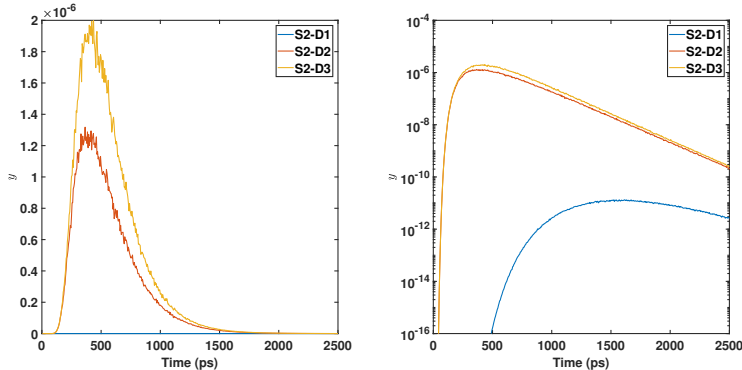


FIGURE 4. Same as Fig. 3 but light is emitted from the source S_2 .

where y_{ijk} and $u(x^j, t^k; x^i; a)$ are given in (2) and (5), respectively. To distinguish, the true value of a is denoted by \bar{a} . We let $F'(a)$ denote the derivative of $F(a)$ with respect to a . We note that the minimization problem of

$$\underset{\xi}{\operatorname{argmin}} \left[\|U - F(a) - F'(a)(a - \xi)\|_2^2 + \lambda \|a - \xi\|_2^2 \right],$$

with the regularization parameter λ is equivalent to the iteration [22, 23]

$$a_{k+1} = a_k + [F'(a_k)^T F'(a_k) + \lambda I]^{-1} F'(a_k)^T (U - F(a_k)). \quad (8)$$

By modifying (8) according to [24], our algorithm of the Levenberg-Marquardt method is described below.

Algorithm 1: Levenberg-Marquardt.

1. Set $k = 0$ and $\lambda = 1$.
2. Calculate $F(a_k)$ and the Jacobian $F'(a_k) = \partial F(a_k) / \partial a_k$.
3. Calculate $S(a_k) = r^T r$, where $r = U - F(a_k)$.

4. Prepare $A = (F'(a_k))^T F'(a_k)$ and $v = F'(a_k)^T r$. Note $A, v \in \mathbb{R}$.
5. Solve $(A + \lambda \text{diag}(A)) \delta = (1 + \lambda) A \delta = -v$.
6. Obtain $S(a_k + \delta)$ and $R = [S(a_k) - S(a_k + \delta)] / [\delta(2v - A\delta)]$.
7. If $R < 0.25$, then set $\nu = 10$ ($\alpha_c < 0.1$), $\nu = 1/\alpha_c$ ($0.1 \leq \alpha_c \leq 0.5$), or $\nu = 2$ ($\alpha_c > 0.5$), where $\alpha_c = [2 - (S(a_k + \delta) - S(a_k)) / \delta v]^{-1}$. If $R < 0.25$ and $\lambda = 0$, set $\lambda = \lambda_c$ and $\nu = \nu/2$, where $\lambda_c = 1/\max(|\text{diag}(A^{-1})_i|) = |A|$. In the case of $R < 0.25$, we finally set $\lambda = \nu\lambda$. If $R > 0.75$, then we set $\lambda = \lambda/2$. If $R > 0.75$ and $\lambda < \lambda_c$, set $\lambda = 0$. Otherwise when $0.25 \leq R \leq 0.75$, no update for λ .
8. If $S(a_k + \delta) \geq S(a_k)$, then return to Step 5.
9. If $S(a_k + \delta) < S(a_k)$, set $a_{k+1} = a_k + \delta$. Then put $k + 1 \rightarrow k$ and go back to Step 2. Repeat the above procedure until one of the stopping criteria $|\delta| < 10^{-4}$ and $S < 10^{-14}$ is fulfilled.

5. INVERSE PROBLEMS BY MARKOV-CHAIN MONTE CARLO

5.1. Bayes formula. Let $f_{\text{prior}}(a)$ be the prior probability density and $L(U|a)$ be a function proportional to the likelihood density. According to the Bayes formula, the conditional probability densities $\pi(a|U)$ is given by

$$\pi(a|U) = \frac{L(U|a)f_{\text{prior}}(a)}{\int_{-\infty}^{\infty} L(U|a)f_{\text{prior}}(a) da}.$$

Since noise is Gaussian, we have

$$L(U|a) = e^{-\frac{1}{2\sigma_e^2} \|U - F(a)\|^2}.$$

In this paper we simply set $f_{\text{prior}}(a) = 1$, which means no a priori knowledge is used for a .

5.2. The Metropolis-Hastings algorithm. Each bin f of the histogram for $\pi(a|U)$ is obtained as

$$f = \int_{-\infty}^{\infty} h(a)\pi(a|U) da,$$

for some $h \in L^1(-\infty, \infty; \pi)$. Suppose

$$a_k \sim \pi(a_k|U), \quad k = 1, 2, \dots, k_{\max}.$$

Then we have

$$f \approx \frac{1}{k_{\max}} \sum_{k=1}^{k_{\max}} h(a_k),$$

for sufficiently large k_{\max} . Using the Metropolis-Hastings algorithm, we can evaluate the above integral even when the normalization factor of $\pi(a|U)$ is not known and only the relation $\pi(a|U) \propto L(U|a)f_{\text{prior}}(a)$ is available.

Let us express $\pi(a|U)$ as

$$p^*(a) = \pi(a|U).$$

We will find $p^*(a)$ using a sequence p_1, p_2, \dots as

$$p^*(a) = \lim_{k \rightarrow \infty} p_k(a).$$

We suppose that $p_{k+1}(a)$ is obtained from $p_k(a)$ (Markov chain) as

$$p_{k+1}(a') = \int_{-\infty}^{\infty} K(a', a)p_k(a) da.$$

We choose the transition kernel $K(a', a)$ so that the desired $p^*(a)$ is obtained in the limit. The transition kernel satisfies

$$K(a', a) \geq 0, \quad \forall a, a' \quad \text{and} \quad \int_{-\infty}^{\infty} K(a', a) da' = 1, \quad \forall a.$$

Let us write $K(a', a)$ as

$$K(a', a) = \alpha(a', a)q(a'|a) + r(a)\delta(a' - a),$$

where

$$r(a) = 1 - \int_{-\infty}^{\infty} \alpha(a', a)q(a'|a) da'.$$

We give the proposal distribution $q(a'|a)$ as

$$q(a'|a) = \mathcal{N}(0, \varepsilon^2),$$

where ε is a parameter. In the numerical calculation below we set

$$\varepsilon = 0.5.$$

We see that the following $\alpha(a', a)$ can be used.

$$\alpha(a', a) = \min \left\{ 1, \frac{\pi(a'|U) q(a|a')}{\pi(a|U) q(a'|a)} \right\}.$$

With the above-mentioned α , the detailed balance is satisfied, i.e.,

$$K(a, a')p(a') = K(a', a)p(a) \Leftrightarrow \alpha(a, a')q(a|a')p(a') = \alpha(a', a)q(a'|a)p(a).$$

Indeed for $p(a')q(a|a') \geq p(a)q(a'|a)$, we have [18]

$$\begin{aligned} \alpha(a', a)q(a'|a)p(a) &= q(a'|a)p(a) \\ &= \frac{p(a)q(a'|a)}{p(a')q(a|a')}q(a|a')p(a') \\ &= \alpha(a, a')q(a|a')p(a'). \end{aligned}$$

A similar calculation holds for $p(a')q(a|a') < p(a)q(a'|a)$.

Suppose that (a_k) is the Metropolis-Hastings Markov chain and moreover the proposal $q(a|a')$ satisfies

$$P[\pi(a_k|U)q(a'|a_k) \leq \pi(a'|U)q(a_k|a')] < 1,$$

which implies that the chain is aperiodic, and $q(a'|a) > 0$ for every $a, a' \in \text{supp } \pi$, which implies irreducibility. Then we have for $h \in L^1(-\infty, \infty; \pi)$ [16]

$$\int_{-\infty}^{\infty} h(a)\pi(a|U) da = \lim_{k_{\max} \rightarrow \infty} \frac{1}{k_{\max}} \sum_{k=1}^{k_{\max}} h(a_k) \quad \text{a.e. } \pi.$$

The Metropolis-Hastings algorithm is summarized below.

Algorithm 2: Metropolis-Hastings.

1. Generate $a' \sim q(\cdot | a_k)$ for given a_k .
2. Generate $\xi \sim \mathcal{U}(0, 1)$ (the uniform distribution).
3. Calculate

$$\alpha(a', a_k) = \min \left\{ 1, \frac{\pi(a'|U)}{\pi(a_k|U)} \frac{q(a_k|a')}{q(a'|a_k)} \right\}.$$

4. Update a_k such that

$$a_{k+1} = \begin{cases} a' & \text{if } \alpha(a', a_k) \geq \xi, \\ a_k & \text{if } \alpha(a', a_k) < \xi. \end{cases}$$

6. TWO-DIMENSIONAL OPTICAL TOMOGRAPHY

6.1. Failure of iterative schemes. We note that

$$\begin{aligned} F'(a) &= \frac{\partial}{\partial a} u(x^j, t^k; x^i; a) \\ &= -3\eta e^{-b_0 t^k} \int_0^{t^k} g(0, t^k; x_{02}, s) g(x_{02}, s; 0, 0) \\ &\quad \times \left(\int_{-\infty}^{\infty} \left[a + 2 \left(1 + \frac{\tanh y_1^2}{10} \right) \right] (1 - \tanh y_1^2) e^{-\frac{(x_1^j - y_1)^2}{4\gamma(t^k - s)}} e^{-\frac{(y_1 - x_1^i)^2}{4\gamma s}} dy_1 \right) ds. \end{aligned}$$

Hence $F'(0) = 0$. For sufficiently small $\epsilon > 0$, we have $F'(\epsilon) > 0$, $F'(-\epsilon) < 0$, $|F'(\pm\epsilon)| \simeq 0$, and $U - F(\pm\epsilon) < 0$. Therefore if we start the iteration from $a_0 = \epsilon$, we obtain

$$|a_1| < \epsilon, \quad |a_2| < |a_1|, \quad \dots$$

Thus the sequence a_k approaches 0 and can never arrive at $a (> 1.1)$.

Let us consider how the norm $\|U - F(a)\|_2$ depends on a . From (5), we have

$$\begin{aligned} U - F(a) &= u(x^j, t^k; x^i; \bar{a})(1 + e_{ijk}) - u(x^j, t^k; x^i; a) \\ &\approx \frac{\eta e^{-b_0 t^k}}{(2\pi\gamma)^2} \int_0^{t^k} \frac{1}{(t^k - s)} e^{-\frac{x_{02}^2}{4\gamma(t^k - s)}} e^{-\frac{x_{02}^2}{4\gamma s}} \\ &\quad \times \left[1 - \frac{\sqrt{\pi\gamma(t^k - s)}}{\ell} e^{\left(\frac{x_{02}}{2\sqrt{\gamma(t^k - s)}} + \frac{\sqrt{\gamma(t^k - s)}}{\ell} \right)^2} \operatorname{erfc} \left(\frac{x_{02}}{2\sqrt{\gamma(t^k - s)}} + \frac{\sqrt{\gamma(t^k - s)}}{\ell} \right) \right] \\ &\quad \times \left[1 - \frac{\sqrt{\pi\gamma s}}{\ell} e^{\left(\frac{x_{02}}{2\sqrt{\gamma s}} + \frac{\sqrt{\gamma s}}{\ell} \right)^2} \operatorname{erfc} \left(\frac{x_{02}}{2\sqrt{\gamma s}} + \frac{\sqrt{\gamma s}}{\ell} \right) \right] \\ &\quad \times \left(\int_{-\infty}^{\infty} d_{\bar{a}}(a, y_1) (1 - \tanh y_1^2) e^{-\frac{(x_1^j - y_1)^2}{4\gamma(t^k - s)}} e^{-\frac{(y_1 - x_1^i)^2}{4\gamma s}} dy_1 \right) ds, \end{aligned}$$

where

$$d_{\bar{a}}(a, y_1) = \bar{a}^2 \left[\bar{a} + 3 \left(1 + \frac{\tanh y_1^2}{10} \right) \right] - a^2 \left[a + 3 \left(1 + \frac{\tanh y_1^2}{10} \right) \right].$$

For a given y_1 , the function $|d_{\bar{a}}(a; y_1)|^2$ has one global minimum at $a = \bar{a}$, one local minimum at $a = -2 \left(1 + \frac{\tanh y_1^2}{10} \right)$, and one local maximum at $a = 0$. Therefore, the above expression of $U - F(a)$ implies that the Levenberg-Marquardt algorithm

fails when the initial value a_0 is negative. Figure 5 shows $|d_{\bar{a}}(a, y_1)|^2$ for $\bar{a} = 1.5$ and $\tanh(y_1^2) = 0.5$.

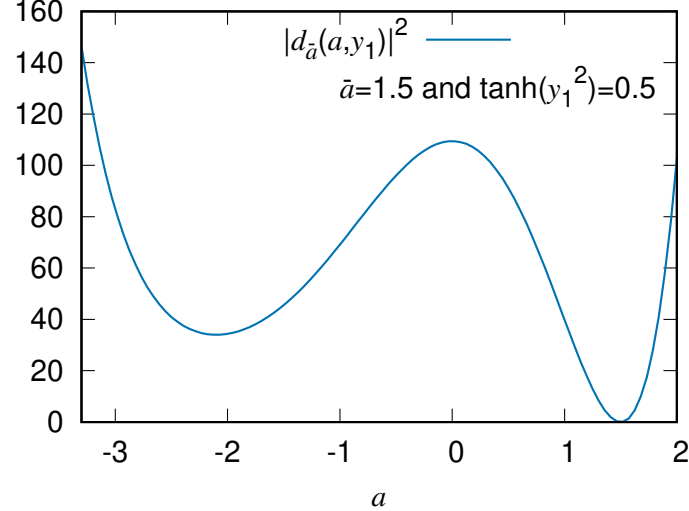


FIGURE 5. The function $|d_{\bar{a}}(a, y_1)|^2$ ($\bar{a} = 1.5$) is plotted when $\tanh(y_1^2) = 0.5$.

Figure 6 shows results from Algorithm 1 (the LM method) for initial guesses $a_0 = -0.1, -0.01$, and 0.01 . When a_0 is negative, the simulation is trapped by the local minimum. The correct value $\bar{a} = 1.5$ is reconstructed for the positive initial guess $a_0 = 0.01$. For numerical calculation, the parameters (6) and (7) are used.

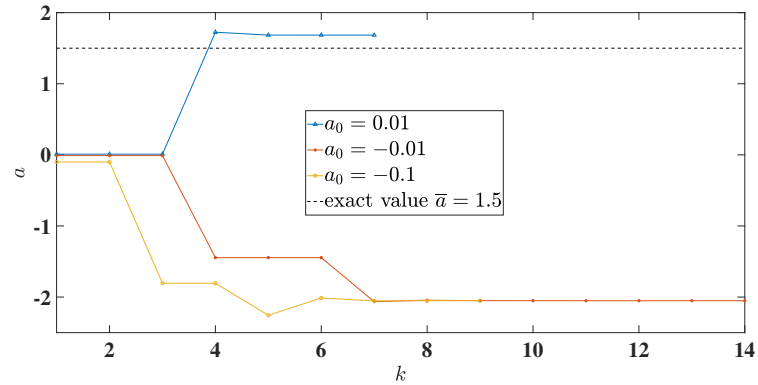


FIGURE 6. Reconstructed \bar{a} with Algorithm 1 (the LM method) for the initial values $a_0 = -0.1$ (blue), $a_0 = -0.01$ (red), and $a_0 = 0.01$ (yellow).

6.2. An MCMC-iterative hybrid method. We show results from Algorithm 2 (the MCMC-MH method) in Figs. 7 and 8. The initial value is set to $a_0 = -0.1$, for which Algorithm 1 fails. We see that obtained values keep fluctuating after burn-in time after escaping the local minimum rather easily. We can recover a by averaging fluctuating values. In Fig. 8, the light blue line shows the average of the obtained a_k from $k = 99$ to $k = 999$, which is 1.6845 with standard deviation 0.11347.

Now we propose to combine Algorithms 1 (the LM method) and 2 (the MCMC-MH method). The procedure of the hybrid algorithm is shown below.

Algorithm 3: Hybrid.

1. Choose an initial guess a_0 , which is not necessarily close to the global minimum.
2. Obtain a reconstructed value a_{k_b} using Algorithm 2.
3. Switch to Algorithm 1 with the initial value a_{k_b} and reconstruct \bar{a} .

At the k_b th MCS (Monte Carlo step) when the calculation arrives at a steady state and starts to fluctuate, we record the obtained reconstructed value a_{k_b} and switch from Algorithm 2 to Algorithm 1 and start the Levenberg-Marquardt algorithm with the initial value the recorded a_{k_b} . After the burn-in time, it is found that we can set $k_b = 99$ in our simulation. This procedure of the hybrid scheme is illustrated in Fig. 9. The correct value of \bar{a} is reconstructed by the proposed hybrid method even when the simulation experiences a local minimum. The initial value $a_{k_b} = 1.8257$ and the simulation stops at $a^* = 1.6841$ ($a^* = a_{k_b+3}$). The reconstructed a^* is not exactly 1.5 due to noise.

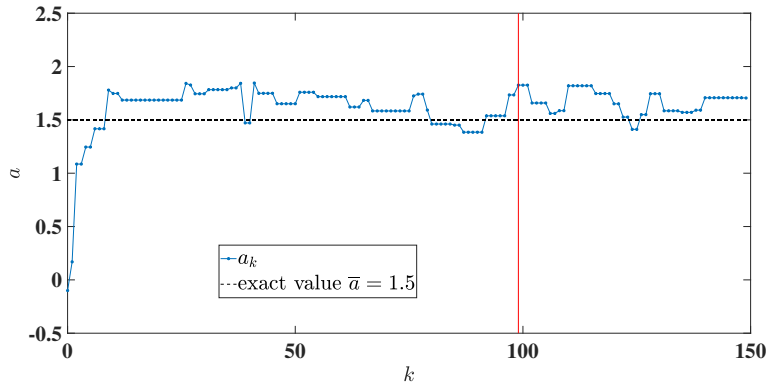


FIGURE 7. Reconstructed \bar{a} with Algorithm 2 (the MCMC-MH method) for the initial value $a_0 = -0.1$.

7. CONCLUDING REMARKS

Practical inverse problems are usually complicated and the cost function has many local minima. As a result, it is not easy to study if the algorithm converges to the global minimum or how the numerical scheme of interest is trapped by local minima. The toy model presented in this paper is simple enough to understand the structure of the cost function, but complicated enough to have one local minimum and one global minimum. In this paper, we used the naive Markov chain Monte

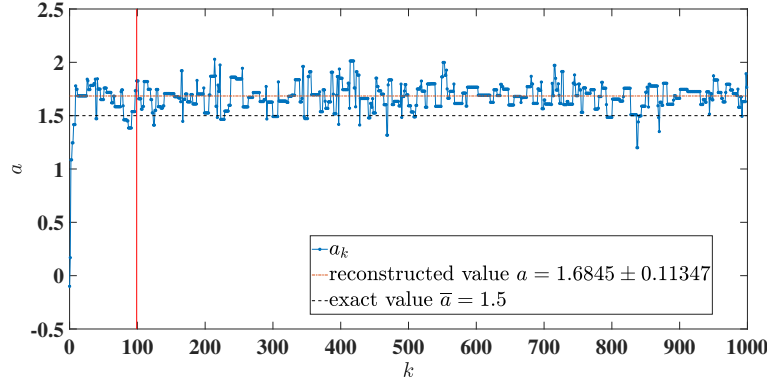


FIGURE 8. Same as Fig. 7 but 1000 values of a_k are shown.

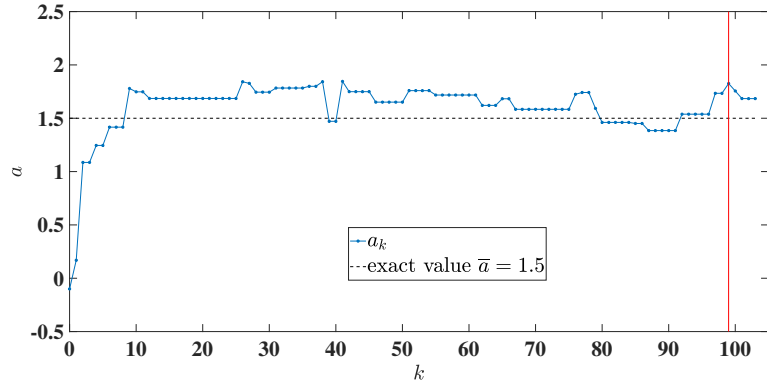


FIGURE 9. Reconstructed \bar{a} with the hybrid scheme of Algorithm 2 and Algorithm 1 for the initial value $a_0 = -0.1$.

Carlo of the Metropolis-Hastings algorithm in order to test the proposed hybrid inversion scheme. In more realistic situations, however, more sophisticated algorithms will be needed. The delayed rejection scheme reduces the net rejection rate [25]. In the adaptive Metropolis algorithm, parameters in the proposal distribution are adjusted during Monte Carlo steps [26]. The DRAM algorithm, which combines the above-mentioned two schemes, was also proposed [27].

ACKNOWLEDGMENT

The authors appreciate Goro Nishimura for fruitful discussion on optical tomography and the use of his computer facilities at Hokkaido University. MM acknowledges support from Grant-in-Aid for Scientific Research (17K05572 and 17H02081) of the Japan Society for the Promotion of Science and from the JSPS A3 foresight program: Modeling and Computation of Applied Inverse Problems. GN was supported by Grant-in-Aid for Scientific Research (15K21766 and 15H05740) of the Japan Society for the Promotion of Science.

APPENDIX A. GREEN'S FUNCTION

The two-dimensional Green's function with the Robin boundary condition can be obtained by extending the formula in [28] derived in one dimension for a pencil incident beam at $t = 0$. As is explained in [29], we can derive an explicit formula for $G(x, t; y, s)$ which satisfies

$$\begin{cases} (\partial_t - \gamma\Delta + b_0) G = \delta(x - y)\delta(t - s), & (x, t) \in \Omega_T, \\ \ell\partial_\nu G + G = 0, & (x, t) \in \partial\Omega_T, \\ G = 0, & x \in \Omega, \quad t = 0, \end{cases}$$

where $(y, s) \in \Omega_T$.

Let us introduce $K(x, t; y, s)$ such that

$$\begin{cases} (\partial_t - \gamma\Delta + b_0) K = \delta(x - y)\delta(t - s), & (x, t) \in \mathbb{R}^2 \times (0, T), \\ K = 0, & x \in \mathbb{R}^2, \quad t = 0, \end{cases}$$

where $(y, s) \in \mathbb{R}^2 \times (0, T)$. Moreover we introduce $G_N(x, t; y, s)$ which satisfies

$$\begin{cases} (\partial_t - \gamma\Delta + b_0) G_N = \delta(x - y)\delta(t - s), & (x, t) \in \Omega_T, \\ \partial_\nu G_N = 0, & (x, t) \in \partial\Omega_T, \\ G_N = 0, & x \in \Omega, \quad t = 0, \end{cases}$$

where $(y, s) \in \Omega_T$. For $t \geq s$, we obtain

$$K(x, t; y, s) = \frac{e^{-b_0(t-s)}}{4\pi\gamma(t-s)} e^{-\frac{|x-y|^2}{4\gamma(t-s)}},$$

and

$$\begin{aligned} G_N(x, t; y, s) &= K(x, t; y_1, y_2, s) + K(x, t; y_1, -y_2, s) \\ &= \frac{e^{-b_0(t-s)}}{4\pi\gamma(t-s)} e^{-\frac{(x_1-y_1)^2}{4\gamma(t-s)}} \left[e^{-\frac{(x_2-y_2)^2}{4\gamma(t-s)}} + e^{-\frac{(x_2+y_2)^2}{4\gamma(t-s)}} \right]. \end{aligned}$$

Furthermore $K = G_N = 0$ for $t < s$. Let us define

$$\phi = G - G_N.$$

We have

$$\begin{cases} (\partial_t - \gamma\Delta + b_0) \phi = 0, & x \in \Omega, \quad t > 0, \\ \ell\partial_\nu \phi + \phi = -G_N, & x \in \partial\Omega, \quad t > 0, \\ \phi = 0, & x \in \Omega, \quad t = 0. \end{cases}$$

We introduce

$$\lambda = \sqrt{\frac{b_0 + p}{\gamma} + q^2}.$$

By the Laplace-Fourier transform given by

$$\hat{\phi}(x_2; p, q; y, s) = \int_0^\infty \int_{-\infty}^\infty e^{-pt} e^{-iqx_1} \phi(x, t; y, s) dx_1 dt,$$

the above diffusion equations are rewritten as

$$\begin{cases} -\frac{d^2}{dx_2^2}\hat{\phi} + \lambda^2\hat{\phi} = 0, & x_2 > 0, \\ -\ell\frac{d\hat{\phi}}{dx_2} + \hat{\phi} = -\hat{G}_N, & x_2 = 0, \end{cases}$$

and

$$-\frac{d^2}{dx_2^2}\hat{K} + \lambda^2\hat{K} = \frac{1}{\gamma}e^{-ps}e^{-iqy_1}\delta(x_2 - y_2), \quad x_2 \in \mathbb{R}.$$

By the Fourier transform with respect to x_2 , we obtain

$$\hat{K}(x_2, y_2) = \frac{1}{2\lambda\gamma}e^{-ps}e^{-iqy_1}e^{-\lambda|x_2-y_2|}.$$

We obtain \hat{G}_N as

$$\begin{aligned} \hat{G}_N(x_2, y_2) &= \hat{G}_N(x_2; p, q; y, s) \\ &= \hat{K}(x_2; p, q; y_1, y_2, s) + \hat{K}(x_2; p, q; y_1, -y_2, s) \\ &= \frac{1}{2\lambda\gamma}e^{-ps}e^{-iqy_1}\left(e^{-\lambda|x_2-y_2|} + e^{-\lambda|x_2+y_2|}\right). \end{aligned}$$

We obtain

$$\begin{aligned} \hat{\phi}(x_2, y_2) &= \frac{-1}{1 + \lambda\ell}\hat{G}_N(0, y_2)e^{-\lambda x_2} \\ &= \frac{-1}{\lambda\gamma(1 + \lambda\ell)}e^{-ps}e^{-iqy_1}e^{-\lambda(x_2+y_2)}. \end{aligned}$$

The following relation can be readily verified.

$$\ell\frac{d}{dy_2}\hat{\phi}(x_2, y_2) - \hat{\phi}(x_2, y_2) = 2\hat{K}(x_2, -y_2), \quad x_2 > 0.$$

Hence we obtain

$$\hat{\phi}(x_2, y_2) = -\frac{2}{\ell}\int_{y_2}^{\infty} e^{(y_2-\xi)/\ell}\hat{K}(x_2, -\xi)d\xi.$$

Therefore,

$$G(x, t; y, s) = G_N(x, t; y, s) - \frac{2}{\ell}\int_{y_2}^{\infty} e^{(y_2-\xi)/\ell}K(x, t; y_1, -\xi, s)d\xi.$$

Thus we arrive at the following solution for $t \geq s$.

$$\begin{aligned} G(x, t; y, s) &= \frac{e^{-b_0(t-s)}}{4\pi\gamma(t-s)}e^{-\frac{(x_1-y_1)^2}{4\gamma(t-s)}}\left[e^{-\frac{(x_2-y_2)^2}{4\gamma(t-s)}} + e^{-\frac{(x_2+y_2)^2}{4\gamma(t-s)}}\right] \\ &\quad - \frac{e^{-b_0(t-s)}}{\ell\sqrt{4\pi\gamma(t-s)}}e^{-\frac{(x_1-y_1)^2}{4\gamma(t-s)}}e^{(x_2+y_2+\beta\gamma(t-s))/\ell} \\ &\quad \times \operatorname{erfc}\left(\frac{x_2+y_2+2\gamma(t-s)/\ell}{\sqrt{4\gamma(t-s)}}\right). \end{aligned}$$

REFERENCES

- [1] R. Choe, A. Corlu, K. Lee, T. Durduran, S. D. Konecky, M. Grosicka-Koptyra, S. R. Arridge, B. J. Czerniecki, D. L. Fraker, A. DeMichele, B. Chance, M. A. Rosen, and A. G. Yodh, *Diffuse optical tomography of breast cancer during neoadjuvant chemotherapy: A case study with comparison to MRI*, *Med. Phys.* **32**, 1128–1139 (2005).
- [2] M. A. Franceschini, D. K. Joseph, T. J. Huppert, S. G. Diamond, and D. A. Boas, *Diffuse optical imaging of the whole head*, *J. Biomed. Opt.* **11**, 054007 (2006).
- [3] David A. Boas, Dana H. Brooks, Eric L. Miller, Charles A. DiMarzio, Misha Kilmer, Richard J. Gaudette, and Quan Zhang, *Imaging the body with diffuse optical tomography*, *IEEE Sign. Process. Mag.* **18**, 57–75 (2001).
- [4] A. P. Gibson, J. C. Hebden, and S. R. Arridge, *Recent advances in diffuse optical imaging*, *Phys. Med. Biol.* **50**, R1–R43 (2005).
- [5] S. R. Arridge, *Methods in diffuse optical imaging*, *Phil. Trans. R. Soc. A* **369**, 4558–4576 (2011).
- [6] S. R. Arridge, *Optical tomography in medical imaging*, *Inverse Problems* **15**, R41–R93 (1999).
- [7] S. R. Arridge and J. C. Schotland, *Optical tomography: forward and inverse problems*, *Inverse Problems* **25**, 123010 (2009).
- [8] M. S. Patterson, B. Chance, and B. C. Wilson, *Time resolved reflectance and transmittance for the non-invasive measurement of tissue optical properties*, *Appl. Opt.* **28**, 2331–2336 (1989).
- [9] A. H. Barnett, J. P. Culver, S. A. Gregory, A. Dale, and D. A. Boas, *Robust inference of baseline optical properties of the human head with three segmentation from magnetic resonance imaging*, *Appl. Opt.* **42**, 3095–108 (2003).
- [10] M Shimada, C. Sato, Y. Hoshi, and Y. Yamada, *Estimation of the absorption coefficients of two-layered media by a simple method using spatially and time-resolved reflectances*, *Phys. Med. Biol.* **54**, 5057–5071 (2009).
- [11] Y. Hoshi, *Towards the next generation of near-infrared spectroscopy*, *Phil. Trans. R. Soc. A* **369**, 4425–4439 (2011).
- [12] Bal G, Langmore I and Marzouk Y 2013 Bayesian inverse problems with Monte Carlo forward models *Inverse Problems and Imaging* **7** 81–105
- [13] Langmore I, Davis A B and Bal G 2013 Multipixel retrieval of structural and optical parameters in a 2-D scene with a path-recycling Monte Carlo forward model and a new Bayesian inference engine *IEEE Trans. Geo. Remote Sensing* **51** 2903–2919
- [14] Arridge S R, Kaipio J P, Kolehmainen V, Schweiger M, Somersalo E, Tarvainen T and Vauhkonen M 2006 Approximation errors and model reduction with an application in optical diffusion tomography *Inverse Problems* **22** 175–195
- [15] Barnett A H, Culver J P, Sorensen A G, Dale A, Boas D A 2003 Robust inference of baseline optical properties of the human head with three-dimensional segmentation from magnetic resonance imaging *Appl. Opt.* **42** 3095–108
- [16] Robert C P and Casella G 1999 *Monte Carlo Statistical Methods* (New York: Springer)
- [17] Liu J S 2004 *Monte Carlo Strategies in Scientific Computing* (New York: Springer)
- [18] Nakamura G and Potthast R 2015 *Inverse Modeling* (Bristol: IOP Publishing)
- [19] Ishimaru A 1978 *Wave Propagation and Scattering in Random Media* (Academic)
- [20] J. B. Keller, *Accuracy and validity of the Born and Rytov approximations*, *J. Opt. Soc. Am.* **59**, 1003–1004 (1969).
- [21] E. Kirklinis, *Renormalization group interpretation of the Born and Rytov approximations*, *J. Opt. Soc. Am. A* **25**, 2499–2508 (2008).
- [22] K. Levenberg, *A method for the solution of certain non-linear problems in least squares*, *Quarterly Appl. Math.* **2**, 164–168 (1944).
- [23] D. Marquardt, *An algorithm for least-squares estimation of nonlinear parameters*, *SIAM J. Appl. Math.* **11**, 431–441 (1963).
- [24] Fletcher R 1971 A modified marquardt subroutine for nonlinear least squares *Rpt. AERE-R 6799*, Harwell
- [25] Tierney L 1994 Markov chains for exploring posterior distributions *Annals of Statistics* **22** 1701–1762
- [26] Haario H, Saksman E and Tamminen J 2001 An adaptive Metropolis algorithm *Bernoulli* **7** 223–242

- [27] Haario H, Laine M, Mira A and Saksman E 2006 DRAM: Efficient adaptive MCMC *Stat. Comput.* **16** 339–354
- [28] Yosida K and Ito S 1976 Functional analysis and differential equations [Japanese] (Tokyo: Iwanami)
- [29] Machida M and Nakamura G arXiv:1706.04500

SCHOOL OF MATHEMATICS, SHANGHAI UNIVERSITY OF FINANCE AND ECONOMICS, SHANGHAI 200433, P.R. CHINA

E-mail address: jiang.yu@mail.shufe.edu.cn

INSTITUTE FOR MEDICAL PHOTONICS RESEARCH, HAMAMATSU UNIVERSITY SCHOOL OF MEDICINE, HAMAMATSU 431-3192, JAPAN

E-mail address: machida@hama-med.ac.jp

DEPARTMENT OF MATHEMATICS, HOKKAIDO UNIVERSITY, SAPPORO 060-0810, JAPAN

E-mail address: nakamuragenn@gmail.com